Validation of the Serpent 2 Monte Carlo code for reactor dosimetry applications

Eric Dorval[1,*]

[1]VTT Technical Research Centre of Finland, P.O. Box 1000, FI-02044, Finland

Abstract. The verification and validation (V&V) of the Serpent 2 Monte Carlo code for 3-D reactor dosimetry applications is being carried out at VTT. Two code-to-code computational benchmark cases were calculated by MCNP and Serpent 2. The computational efficiency of different variance reduction techniques was appraised. The validation part currently includes two experimental benchmarks from the SINBAD database: the Pool Critical Assembly-Pressure Vessel Facility (PCA); and the H.B. Robinson-2 (HBR-2) Pressure Vessel Dosimetry Benchmark. All simulations replicate the benchmark source specifications at pin level thanks to the development of a flexible, geometry-independent, fixed source definition for reactor dosimetry applications. Good agreement was found in all benchmark cases.

1 Introduction

The Serpent 2 Monte Carlo code [1] was originally targeted at lattice physics applications. Subsequent developments have extended its capabilities to full-core calculations, photon transport, activation and shielding. The V&V of Serpent applied to reactor dosimetry is being carried out mainly following the guidelines of the U.S. NRC Regulatory Guide 1.190 [2], which prescribes code-to-code calculational benchmarks as well as comparisons with benchmark measurements.

Two PWR verification cases were selected: a specification with Standard Core Loading Pattern (STD); and a Partial Length Shield Assembly (PLS) core [3]. Fast fluxes were calculated with MCNP [4] version 6.1 and Serpent 2, based on identical geometry and material definitions. The present validation comprises two experimental benchmarks: the PCA Pressure Vessel Facility; and the HBR-2 Vessel Dosimetry Benchmark. Detailed Serpent models were setup for the calculation of selected dosimetry reaction rates using cross section (XS) data from IRDFF [5] version 1.05.

* Corresponding author: eric.dorval@vtt.fi1)

2 Methods

2. 1 Fixed neutron source routines for reactor dosimetry applications

In-house modifications were made to the Serpent code (version 2.1.32) to allow fixed neutron source definitions of practical interest for reactor dosimetry. Source specifications are read from an external text file containing all the parameters needed by Serpent to sample source points that replicate the degree of detail/complexity imposed by the benchmarks. Sources from different core simulators for diverse reactor core types can be generated by using the appropriate format setup of this external file. Source points are sampled at two levels: assembly and pin. The fixed source specification is independent of the geometry definition. Table 1 summarizes the fixed neutron source features.

Table 1: Fixed neutron source options available in the new routines. Axial distributions may have different axial discretization per assembly. Energy distributions can be combined freely.

1st level (assembly)	2nd level (pin)	Pin type	Axial	Angular	Energy
Cartesian, hexagonal	Cartesian, hexagonal	square, (hollow) cylindrical, rectangular, (bent) MTR plate	piece-wise constant	isotropic	histogram, Watt fission spectrum, Maxwell fission spectrum

2.2 Benchmarks

Benchmark descriptions are left outside this article due to size considerations. The interested reader is referred to the appropriate documentation. Here, only the most salient features, assumptions and other indispensable information related to the solution method are given. Figure 1 (upper row) depicts top views of the reactor models studied in this work, whereas Figure 1 (bottom row) shows the corresponding importance maps generated with the built-in response matrix solver of Serpent [6] for the same cases.

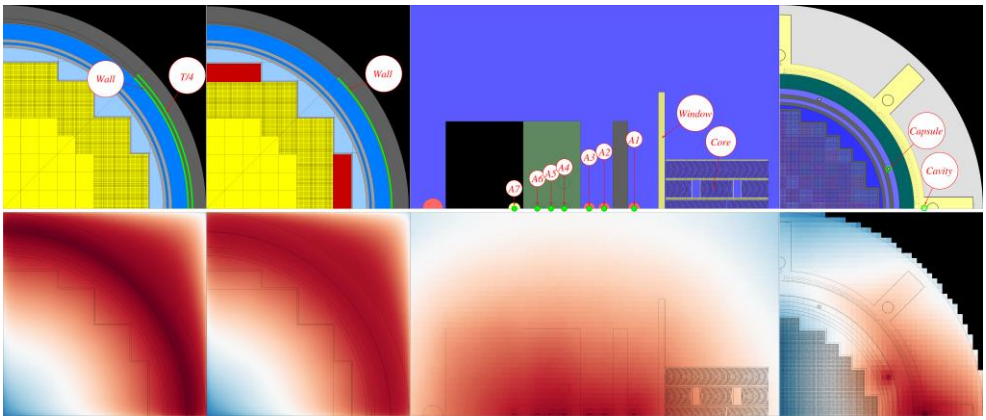

Figure 1: Top views of the Serpent models used in this work. From left to right: STD; PLS; PCA (partial extents); and HBR-2. Bottom row: detector importance maps. Neutron importance increases from the blue tones toward the red ones. Figures are not to scale.

The importances calculated by Serpent's built-in deterministic solver are inversely proportional to the lower weight bounds used in weight windows. Importance maps should not be confused with *cell importances* (as in MCNP). Although Serpent can handle cell importances, importance maps are the way in which Serpent implements weight windows.

2.2.1 Computational benchmarks

MCNP input files of the STD and PLS numerical benchmark problems were facilitated by one of the authors of NUREG/CR-6115 [3]. Corresponding Serpent inputs were created from scratch. In addition to identical geometry, material, and fixed source definitions, the Serpent 2 models also feature the same Variance Reduction (VR) techniques used in Ref. [3], namely *cell importances* and energy cut-off. The adoption of *cell importances* increases the complexity of the geometry definition because it necessitates individual cells where the *cell importances* are set. This can be observed in the peripheral assemblies of the leftmost pictures in Figure 1 (left).

While the original models from NUREG/CR-6115 were based on multi-group cross section (XS) neutron transport libraries, this work was carried out with the continuous energy library ENDF/B-VII.1. Fast (E > 1 MeV) neutron fluxes computed by MCNP version 6.1 at two axial locations ("Peak" and "Weld") were taken as a reference solution. Given the vast number of fluxes to be compared, the agreement between Serpent and MCNP solutions is reported in the form of reduced chi-squared values:

$$\frac{\chi^2}{DOF} = \frac{1}{n}\sum_{i=1}^{n}\frac{(s_i - m_i)^2}{\sigma_i^2}\,, \tag{1}$$

where s_i and m_i denote the Serpent and MCNP results, respectively; n is the number of results, or degrees of freedom (DOF); and σ_i is an appropriate measure of combined uncertainty between MCNP and Serpent ($\sigma_{m,i}$ and $\sigma_{s,i}$, respectively):

$$\sigma_i = \sqrt{\sigma_{m,i}^2 + \sigma_{s,i}^2}\,. \tag{2}$$

Additional STD and PLS cases not present in Ref. [3] were calculated with Serpent. In these, the VR was switched from *cell importances* to one-group weight windows (WWs) generated by Serpent. Since the new source routines in Serpent do not require explicit definition of the geometry at pin level, yet two more additional cases were run, where every fuel assembly was represented as a single cell, whilst still retaining the full detail of the pin-wise source dependence. The aim of the latter cases is to quantify the computational overheads associated with the definition of unnecessary additional cells and the use of surface-tracking instead of delta-tracking [7]. The overheads are quantified through the figure of merit (FOM), defined for a given tally as:

$$FOM = \frac{1}{\sigma^2 T}\,, \tag{3}$$

where T is the total computation time, and σ is the mean absolute statistical uncertainty of all azimuthal detector locations considered: $\sigma = \widetilde{\sigma_{s,i}}$.

2.2.2 PCA

The first experimental case of this work is the PCA Pressure Vessel Wall Facility Benchmark Configuration 12/13 [8,9], which features a fresh, highly enriched (93 %), materials testing reactor (MTR) core with 18 bent fuel plates per standard fuel element. The benchmark in SINBAD [10] includes experimental data for six nuclear reactions at seven

ex-core locations in water, carbon steel, and air. Dosimeter locations denoted by "A1" ... "A7" are defined along the core horizontal centreline. The numbering increases with the distance to the PCA window. This window is situated to the left of the core (Figure 1, centre picture).

Two simplifications were introduced in the Serpent model: control rods (CRs) were not explicitly represented; and all fuel elements were modelled with 18 fuel plates (except for those with CR channels). The first assumption is well justified, since the fixed neutron source is a part of the benchmark specification, whereas the effect of the second simplification is expected to be small, because the fuel meat densities were adjusted to match the actual ^{235}U mass in elements with either 17 or 19 plates. This change was driven by the current implementation of the fixed source routine in Serpent, which is limited to the same number of pins (or plates) per assembly (element) at the 2nd level in Table 1.

The Serpent model was run using two neutron transport nuclear data libraries, namely ENDF/B-VII.1 [11] and JEFF-3.1.2 [12]. An unperturbed Watt fission spectrum of thermal neutrons on ^{235}U was adopted. Dosimetry XS data from IRDFF version 1.05 was used. One-group WWs were generated by Serpent. The results are presented in the form of calculated-to-experimental (C/E) reaction rate ratios per isotope and per location.

2.2.3 HBR-2

The HBR-2 benchmark [13] is the most complex one studied in this work. The complexity stems from the pin-wise nature of the neutron source produced by a core simulator, the time-dependence of the global (proportional to total power) and local (spatial) neutron source distributions, and the number of structural components. The SINBAD database [14] provides nine full-core, pin-wise neutron source specifications: one for cycle-average conditions; and others at eight selected time steps during cycle 9.

The Serpent model features explicit heterogeneous fuel elements with axially-uniform burnup distributions at mid-cycle conditions. Fuel inventories were calculated also with Serpent, based on a simplified, 2-D single-assembly model. This auxiliary depletion calculation supplied the data necessary to setup the neutron source rigorously, i.e., to allow sampling of isotope-dependent fission spectra weighted with the number of emitted neutrons, as opposed to fission fractions. Moreover, this source treatment provided estimates of the neutron source strength as a function of the cycle step. The neutron emission energies were sampled from Watt fission spectra corresponding to ^{235}U, ^{238}U and ^{239}Pu. The relative contributions varied according to the assembly exposure.

The VR techniques used were energy cut-off and one-group WWs. Dosimetry and transport XS data were taken from the IRDFF and ENDF/B-VII.1 library, respectively. The results of the benchmark are supplied in the form of C/E activity ratios per isotope as a function of the dosimetry location (surveillance capsule or cavity) for the three approaches adopted to cater for neutron sources during cycle 9, to be described in the Results section.

3 Results

3. 1 Computational benchmarks

Fast neutron fluxes calculated by MCNP and by Serpent are depicted in Figure 2. There is evidence of very good agreement when Serpent uses the same VR techniques as MCNP, namely *cell importances* and energy cut-off. This scenario is labelled as "**Case A**". Two

additional scenarios were simulated with Serpent only: in **Case B**, *cell importances* were replaced by weight windows. In **Case C**, the geometry was simplified by merging all peripheral pin cells into single assembly cells; delta-tracking and weight windows were used. Table 2 summarizes the results for all the cases by reporting reduced chi-squared values through Equation (1) and FOMs via Equation (3) for the Serpent cases only.

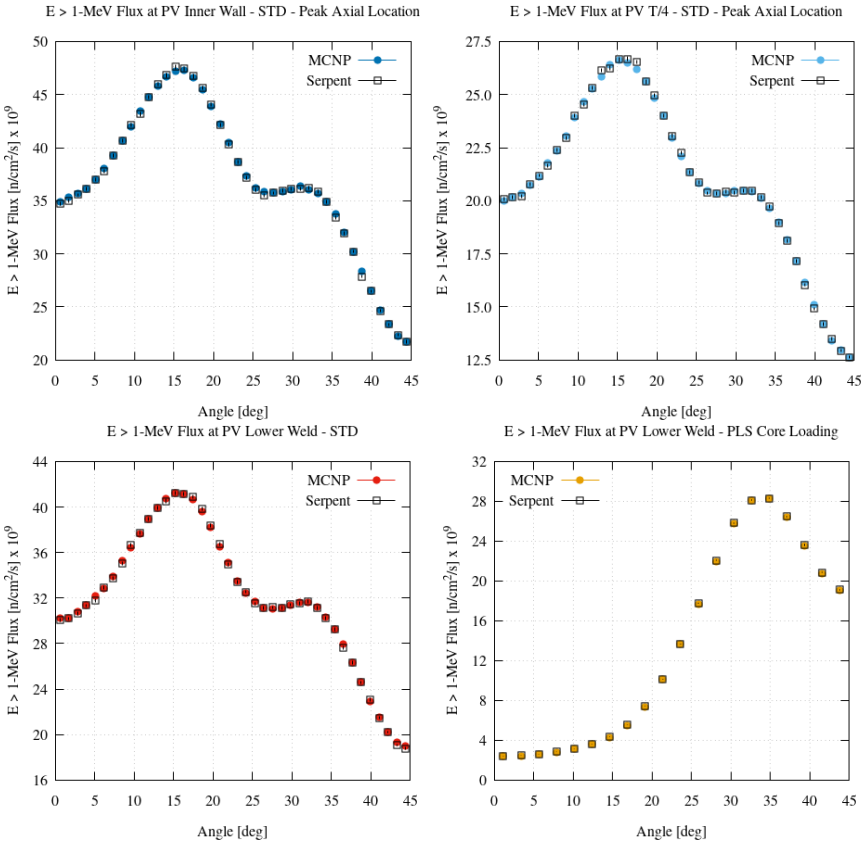

Figure 2: Fast neutron fluxes (and their statistical uncertainties) at various locations for the STD and PLS computational benchmarks using identical geometry and VR techniques (**Case A**).

In general, reduced χ^2 values in the interval [0.3, 2.0] are evidence of good statistical agreement. All combinations of geometry definitions, tracking and VR techniques yield results comparable to those of MCNP. The FOM values of **Cases B** and **C** underline the higher computational efficiency of WWs against *cell importances* for this case, as well as the improvements brought about by the geometry simplifications and delta-tracking.

Table 2: Reduced χ^2 and FOM for computational benchmarks. Azimuthal fast neutron flux profiles were calculated at the Pressure Vessel (PV) Lower Weld, Inner Wall, and fourth thickness (T/4).

Result	**Case A**		**Case B**		**Case C**	
	χ^2/DOF	FOM	χ^2/DOF	FOM	χ^2/DOF	FOM
STD PV Lower Weld	0.9	11	1.2	65	0.6	123
STD PV Inner Wall – Peak	1.2	47	1.0	248	1.0	452
STD T/4 – Peak	0.8	15	1.6	79	0.9	148
PLS Lower Weld	1.7	316	0.3	449	0.8	1542

3.2 Experimental benchmarks

3.2.1 Pool Critical Assembly – Pressure Vessel Facility Benchmark

Figure 3, Table 3 and Table 4 present the C/E reaction rate ratios along with their statistical uncertainties, which are largely governed by the experimental data. The overall agreement of Serpent results with experiments is very satisfactory. No significant differences based on the adoption of either ENDF/B-VII.1 or JEFF-3.1.2 data are evident. The high uncertainty from the ^{237}Np dosimeter at location A7 stems from the measurements (8.4 %).

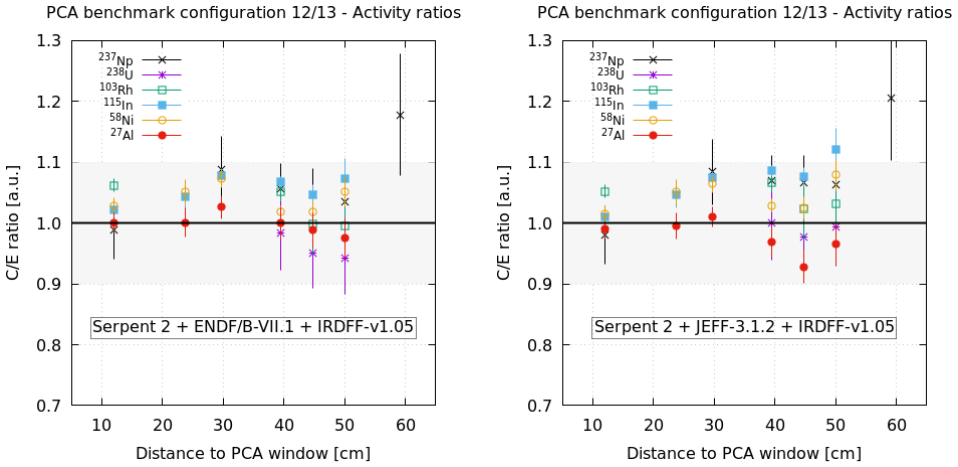

Figure 3: Specific activity C/E ratios for the PCA case. Calculations with Serpent 2 were conducted using transport XS data from ENDF/B-VII.1 (left) and JEFF-3.1.2 libraries (right). Both cases use the same dosimetry XS data (IRDFF version 1.05). Shaded areas represent a ± 10 % uncertainty range.

Table 3: C/E specific activity ratios for the PCA benchmark problem. Uncertainties of averages are based on observed sample standard deviations only. Transport XS data from ENDF/B-VII.1.

Location / Distance (cm)	ENDF/B-VII.1 XS data											
	^{237}Np(n,f)^{137}Cs		^{238}U(n,f)^{137}Cs		^{103}Rh(n,n')^{103m}Rh		^{115}In(n,n')^{115m}In		^{58}Ni(n,p)^{58}Co		^{27}Al(n,α)^{24}Na	
	C/E	**unc**	**C/E**	**unc**	**C/E**	**unc**	**C/E**	**unc**	**C/E**	**unc**	**C/E**	**unc**
A1 / 12.0	0.99	0.05	-	-	1.06	0.01	1.02	0.01	1.03	0.01	1.00	0.01
A2 / 23.8	-	-	-	-	-	-	1.04	0.02	1.05	0.02	1.00	0.02
A3 / 29.7	1.09	0.05	-	-	-	-	1.08	0.01	1.07	0.02	1.03	0.02
A4 / 39.5	1.06	0.04	0.98	0.06	1.05	0.02	1.07	0.01	1.02	0.01	1.00	0.03
A5 / 44.7	1.05	0.04	0.95	0.06	1.00	0.05	1.05	0.02	1.02	0.02	0.99	0.03
A6 / 50.1	1.03	0.05	0.94	0.06	1.00	0.05	1.07	0.03	1.05	0.02	0.98	0.03
A7 / 59.1	1.18	0.10	-	-	-	-	-	-	-	-	-	-
Average	**1.07**	**0.06**	**0.96**	**0.02**	**1.03**	**0.03**	**1.06**	**0.02**	**1.04**	**0.02**	**1.00**	**0.02**

Table 4: C/E specific activity ratios for the PCA benchmark problem. Uncertainties of averages are based on observed sample standard deviations only. Transport XS data from JEFF-3.1.2.

Location / Distance (cm)	JEFF-3.1.2 XS data											
	^{237}Np(n,f)^{137}Cs		^{238}U(n,f)^{137}Cs		^{103}Rh(n,n')^{103m}Rh		^{115}In(n,n')^{115m}In		^{58}Ni(n,p)^{58}Co		^{27}Al(n,α)^{24}Na	
	C/E	**unc**	**C/E**	**unc**	**C/E**	**unc**	**C/E**	**unc**	**C/E**	**unc**	**C/E**	**unc**
A1 / 12.0	0.98	0.05	-	-	1.05	0.01	1.01	0.01	1.01	0.01	0.99	0.01
A2 / 23.8	-	-	-	-	-	-	1.05	0.02	1.05	0.02	0.99	0.02
A3 / 29.7	1.08	0.05	-	-	-	-	1.07	0.01	1.07	0.02	1.01	0.02
A4 / 39.5	1.07	0.04	1.00	0.06	1.07	0.02	1.09	0.01	1.03	0.01	0.97	0.03
A5 / 44.7	1.07	0.05	0.98	0.06	1.02	0.05	1.08	0.02	1.03	0.02	0.93	0.03
A6 / 50.1	1.06	0.05	0.99	0.06	1.03	0.05	1.12	0.03	1.08	0.03	0.96	0.03
A7 / 59.1	1.21	0.10	-	-	-	-	-	-	-	-	-	-
Average	**1.08**	**0.07**	**0.99**	**0.01**	**1.04**	**0.02**	**1.07**	**0.04**	**1.04**	**0.03**	**0.98**	**0.03**

3.2.2 H.B. Robinson-2 Pressure Vessel Dosimetry Benchmark

Table 5 summarizes the C/E activity ratios at the capsule and cavity locations, respectively. These locations are depicted by green dots in Figure 1 (right). The three cases reported per location differ in how the time-dependence of the neutron source was accounted for. All three cases account for variations in reactor power when calculating activities. In **Case 1** and **Case 2**, a single transport calculation was executed. In **Case 2**, reaction rates were corrected based on the power of the peripheral fuel assemblies at eight time-steps, as done somewhere else [13,14]. **Case 3** is the result of post-processing eight different Serpent runs, each one featuring a distinctive neutron source as supplied in the benchmark specification: atomic reaction rates from Serpent runs were associated with their corresponding irradiation history intervals. Then, decay-corrected activities in units of Bq/mg were obtained.

Table 5: C/E ratios of activities at End-of-Irradiation (EoI) in HBR-2 benchmark. Averages report sample standard deviations only. Uncertainties below 0.5 % read "0.00".

Reaction	Capsule						Cavity					
	Case 1		**Case 2**		**Case 3**		**Case 1**		**Case 2**		**Case 3**	
	C/E	**unc**	**C/E**	**unc**	**C/E**	**unc**	**C/E**	**unc**	**C/E**	**unc**	**C/E**	**unc**
^{237}Np(n,f)^{137}Cs	1.00	0.00	0.98	0.00	0.97	0.00	0.85	0.00	0.81	0.00	0.81	0.00
^{238}U(n,f)^{137}Cs	0.97	0.00	0.95	0.00	0.94	0.00	0.94	0.00	0.90	0.00	0.91	0.00
^{58}Ni(n,p)$^{58m+g}$Co	0.96	0.00	1.01	0.00	0.97	0.00	0.85	0.01	0.94	0.01	0.93	0.02
^{54}Fe(n,p)^{54}Mn	1.01	0.00	1.02	0.00	1.00	0.00	0.97	0.01	0.97	0.01	0.98	0.01
^{46}Ti(n,p)^{46}Sc	1.02	0.00	1.06	0.00	1.03	0.00	0.95	0.01	1.04	0.01	1.02	0.02
^{63}Cu(n,α)^{60}Co	1.05	0.01	1.04	0.01	1.03	0.00	1.02	0.02	0.98	0.02	0.98	0.01
Average	**1.00**	0.00	**1.01**	0.00	**0.99**	0.00	**0.93**	0.01	**0.94**	0.01	**0.94**	0.01
(without ^{237}Np)	**1.00**	0.00	**1.02**	0.00	**0.99**	0.00	**0.95**	0.01	**0.96**	0.01	**0.96**	0.01

In all cases, the agreement with experiments is satisfactory, and there is no evidence of drastic improvements when opting for either **Case 2** or **Case 3**, except for the reaction ^{58}Ni(n,p)$^{58m+g}$Co. It is worthwhile mentioning that the results reported in this work only include the (propagated) statistical uncertainties in Serpent tallies, since the benchmark does not report experimental uncertainties. Corrections due to photo-fission and activation

of impurities were applied to the experimental data prior to its comparison against calculations. Average results are presented with and without the contribution of the $^{237}Np(n,f)^{137}Cs$ reaction, since there likely is an error in the measured ^{137}Cs activities [13].

4 Conclusions

A systematic V&V of the Serpent 2 Monte Carlo applied to reactor dosimetry is being carried out according to U.S. NRC guidelines. Thus far, two computational and two experimental benchmark models were analysed, yielding good agreement with reference data. The models include a high degree of detail, and it is envisaged that they could be used as a basis for future studies. In particular, special effort was invested in the development of fixed source routines in Serpent that could match as closely as possible the dosimetry benchmark specifications. Some of the cases studied allowed quantifying the effect of variance reduction techniques and modelling practices on computational efficiency. The insights gained during this work will be applied in the upcoming benchmark calculations to continue the verification and validation of Serpent 2.

Gabriel Zamonksy is dearly acknowledged for supplying the MCNP inputs (including neutron source specifications) for the PLS and STD cases. This work was funded by the Finnish Research Programme on Nuclear Power Plant Safety SAFIR2022/RACSA project.

References

1. J. Leppänen, M. Pusa, T. Viitanen, V. Valtavirta, and T. Kaltiaisenaho, Ann. Nucl. Energy **82**, pp. 142-150 (2015)
2. U.S. Nuclear Regulatory Commission, *Regulatory Guide 1.190* (2001)
3. J. Carew, K. Hu, A. Aronson, A. Prince, and G. Zamonsky, NUREG/CR-6115 (2001)
4. D. B. Pelowitz (Ed.), *MCNP6™ User's Manual*, LA-CP-13-00634 Rev. 0 (2013)
5. E. Zsolnay, R. Capote Noy, H. Nolthenius, and A. Trkov, INDC(NDS)-0616 (2012)
6. J. Leppänen, Nucl. Technol **205** (11), pp. 1416-1432 (2019).
7. J. Leppänen, Ann. Nucl. Energy **37**, pp. 715-722 (2010)
8. I. Remec and F. Kam, NUREG/CR-6454 (1997)
9. W. McElroy (Ed.), NUREG/CR-1861 (1981)
10. I. Kodeli, E. Sartori, and B. Kirk, Proc. Am. Nuc. Soc. 14th Topical Meeting of the Radiation Protection and Shielding Division (2006)
11. National Nuclear Data Center (NNDC), ENDF/B-VII.1 Evaluated Nuclear Data Library, Brookhaven National Laboratory (2011)
12. Nuclear Energy Agency (NEA), Joint Evaluated Fission and Fusion nuclear data library JEFF-3.1.2 (2016)
13. I. Remec and F. Kam, NUREG/CR-6453 (1997)
14. R. Orsi, Nucl. Eng. Technol.**52** (2), pp. 448-455(2020)